INVESTIGATION OF THE RELATIONSHIP BETWEEN FORMATION FACTOR AND FRESH PROPERTIES OF CONCRETE

FINAL PROJECT REPORT

by

O. Burkan Isgor[1], Hossein Sallehi[2], and Pouria Ghods[2]
[1]Oregon State University, [2]Carleton University

Sponsorship
The Pacific Northwest Transportation Consortium (PacTrans)
Natural Sciences and Engineering Research Council of Canada (NSERC)

for
Pacific Northwest Transportation Consortium (PacTrans)
USDOT University Transportation Center for Federal Region 10
University of Washington
More Hall 112, Box 352700
Seattle, WA 98195-2700

In cooperation with US Department of Transportation-Research and Innovative Technology Administration (RITA)

Disclaimer

The contents of this report reflect the views of the authors, who are responsible for the facts and the accuracy of the information presented herein. This document is disseminated under the sponsorship of the U.S. Department of Transportation's University Transportation Centers Program, in the interest of information exchange. The Pacific Northwest Transportation Consortium, the U.S. Government and matching sponsor assume no liability for the contents or use thereof.

Technical Report Documentation Page

1. Report No.	2. Government Accession No.	3. Recipient's Catalog No.

4. Title and Subtitle	5. Report Date
Investigation of the relationship between formation factor and fresh properties of concrete	11/30/2017
	6. Performing Organization Code

7. Author(s)	8. Performing Organization Report No.
O. Burkan Isgor, Hossein Sallehi, Pouria Ghods	

9. Performing Organization Name and Address	10. Work Unit No. (TRAIS)
PacTrans Pacific Northwest Transportation Consortium University Transportation Center for Region 10 University of Washington More Hall 112 Seattle, WA 98195-2700	**11. Contract or Grant No.**

12. Sponsoring Organization Name and Address	13. Type of Report and Period Covered
United States of America Department of Transportation Research and Innovative Technology Administration	**14. Sponsoring Agency Code**

15. Supplementary Notes

Report uploaded at www.pacTrans.org

16. Abstract

Formation factor of fresh cementitious pastes was investigated experimentally as a function of time from initial mixing and mixture design properties such as supplementary cementitious material (SCM) replacement level, water-to-binder ratio (w/cm), and superplasticizer dosage. SCM types included fly ash, slag and silica fume. A total of 54 paste mixtures were studied. The formation factor of each fresh paste was determined at the 30th, 60th, and 90th minutes from initial mixing. It was shown that for a given type of paste mixture (e.g. OPC plus silica fume), formation factor decreases if porosity or w/cm ratio increases, and this relationship can be well formulized by a power function. Although both paste and pore solution resistivity decrease with time in fresh cement paste mixtures until initial setting, their ratio (formation factor) remains relatively constant because it is only indicative of physical formation of solid particles in the pore solution. Formation factor of fresh cement paste is strongly correlated to its porosity through Archie's law, which implies that formation factor decreases if porosity increases. This decrease of formation factor is attributed to the smaller solid particles fraction (i.e., 1-φ) with high resistivity (i.e., lower amount of non-conductive component compared to conductive component). The tortuosity of paste affects the formation factor even at a constant porosity. Smaller size, angular shape, and more even distribution of particles increase the tortuosity of the paste. Slag and fly ash particles considerably decrease tortuosity; whereas silica fume incorporated pastes have almost the same tortuosity as OPC pastes. Superplasticizer addition significantly increases tortuosity through a better distribution of solid particles.

17. Key Words	18. Distribution Statement
Cement; supplementary cementitious materials; fresh concrete; formation factor; electrical resistivity.	No restrictions.

19. Security Classification (of this report)	20. Security Classification (of this page)	21. No. of Pages	22. Price
Unclassified.	Unclassified.		NA

Form DOT F 1700.7 (8-72) **Reproduction of completed page authorized**

Table of Contents

List of Figures

List of Tables

Acknowledgments

The authors would like to thank the Natural Sciences and Engineering Research Council of Canada (NSERC) and the Pacific Northwest Transportation Consortium (PacTrans) for their financial support. We also would like to acknowledge Dr. Rahil Khoshnazar, Dr. Vahid Jafari Azad, and Tyler Deboodt for her technical support throughout the project.

Executive Summary

Construction projects using ready mix concrete require strict adherence to the established standards for specifying, ordering, mixing, delivering and curing; however, many newly constructed structures suffer from performance and long-term durability problems due to low-quality concrete. The issue can be traced back to existing quality control (QC) and quality assurance (QA) protocols of concrete production, which mainly require the measurement of slump, unit weight and air content of fresh concrete. While these measurements have value, they do not provide direct links to long-term performance and durability indicators such as water content, porosity, strength or transport properties. The absence of a QC protocol that directly assesses performance at the time of delivery is a major limitation for the construction industry. Similarly, current QA procedures have drawbacks as they mainly rely on checking compressive strength of concrete, which is typically done weeks after concrete placement. This approach poses practical challenges in terms of the timing of the QA decisions, and it does not necessarily provide adequate information about the future performance of structures in terms of their durability because it mainly checks if the desired mechanical properties are satisfied.
There is a need for improved and practical QC/QA protocols (1) to confirm that the fresh concrete delivered to the site is the concrete that is specified, ordered, and delivered to the construction site, (2) to ensure that the delivered fresh concrete mixture will satisfy the performance specifications for long-term durability.

Formation factor of fresh concrete is proposed as a parameter to address these two demands and to supplement existing QC/QA protocols. Although it has been shown in past research that formation factor of hardened concrete can be used to predict long-term durability properties of concrete; the formation factor of fresh concrete has not been systematically

investigated. This research aims to fill this gap by studying the formation factor of neat and blended cementitious materials in fresh state as a function of time from initial mixing and mixture design properties such as supplementary cementitious material (SCM) replacement level, water-to-binder ratio (w/cm), and superplasticizer dosage.

Formation factor of fresh cementitious pastes was investigated experimentally as a function of time from initial mixing and mixture design properties such as supplementary cementitious material (SCM) replacement level, water-to-binder ratio (w/cm), and superplasticizer dosage. SCM types included fly ash, slag and silica fume. A total of 54 paste mixtures were studied. The formation factor of each fresh paste was determined at the 30th, 60th, and 90th minutes from initial mixing. It was shown that for a given type of paste mixture (e.g. OPC plus silica fume), formation factor decreases if porosity or w/cm ratio increases, and this relationship can be well formulized by a power function. Although both paste and pore solution resistivity decrease with time in fresh cement paste mixtures until initial setting, their ratio (formation factor) remains relatively constant because it is only indicative of physical formation of solid particles in the pore solution. Formation factor of fresh cement paste is strongly correlated to its porosity through Archie's law, which implies that formation factor decreases if porosity increases. This decrease of formation factor is attributed to the smaller solid particles fraction (i.e., 1-φ) with high resistivity (i.e., lower amount of non-conductive component compared to conductive component). The tortuosity of paste affects the formation factor even at a constant porosity. Smaller size, angular shape, and more even distribution of particles increase the tortuosity of the paste. Slag and fly ash particles considerably decrease tortuosity; whereas silica fume incorporated pastes have almost the same tortuosity as OPC pastes. Superplasticizer addition significantly increases tortuosity through a better distribution of solid particles.

Chapter 1 Introduction

1.1 Introduction

Each year approximately 10 billion tons of concrete is produced, making concrete the largest manufactured product globally [1]. The majority of this production is in the form of ready mix concrete [2]. In the United States alone, there are about 5,500 ready mix concrete plants and about 55,000 ready mixed concrete mixer trucks that deliver concrete to the point of placement [2]. The quality control (QC) and quality assurance (QA) of this large operation have major economic, social and environmental implications. Construction projects using ready mix concrete require strict adherence to the established standards for specifying, ordering, mixing, delivering and curing, such as those defined by ASTM C94 [3], the Standard Specification for Ready-Mixed Concrete. Despite all efforts and streamlined procedures, many newly constructed structures suffer from performance and long-term durability problems due to low-quality concrete.

The issue can be traced back to existing QC/QA protocols of concrete production. Current QC protocols require the measurement of slump, unit weight and air content of fresh concrete [3]. While these measurements have value, they do not provide direct links to long-term performance and durability indicators such as water content, porosity, strength or transport properties. The absence of a QC protocol that directly assesses performance at the time of delivery is a major limitation for the construction industry. Similarly, current QA procedures have drawbacks as they mainly rely on checking compressive strength of concrete, which is typically done weeks after concrete placement. This approach poses practical challenges in terms of the timing of the QA decisions, and it does not necessarily provide adequate information about

the future performance of structures in terms of their durability because it mainly checks if the desired mechanical properties are satisfied.

There is a need for improved and practical QC/QA protocols (1) to confirm that the fresh concrete delivered to the site is the concrete that is specified, ordered, and delivered to the construction site, (2) to ensure that the delivered fresh concrete mixture will satisfy the performance specifications for long-term durability. Formation factor of fresh concrete is proposed as a parameter to address these two demands and to supplement existing QC/QA protocols. Although it has been shown in past research that formation factor of hardened concrete can be used to predict long-term durability properties of concrete [4-15]; the formation factor of fresh concrete has not been systematically investigated. This papers aims to fill this gap by studying the formation factor of neat and blended cementitious materials in fresh state as a function of time from initial mixing and mixture design properties such as supplementary cementitious material (SCM) replacement level, water-to-binder ratio (w/cm), and superplasticizer dosage.

Chapter 2 Literature Review

Porosity in a porous material such as rocks or soils is defined as the volumetric ratio of air voids and water to the total material (i.e., solid, air and water). In a fresh cement paste, all air voids (pores) are mostly filled with water, hence, the degree of saturation can be assumed 100%. Therefore, the volume of water is equal to that of air voids, and porosity in a cement paste is defined as the volumetric ratio of water content to that of water plus cementitious materials. As shown in Fig. 2.1, the porosity is the ratio of the space free of cementitious materials (white area) to the total volume (shaded area plus white area). As a result, increasing water content in unit volume of cement paste (i.e., higher w/cm ratio) will result in higher porosity [13, 16]. Electrical resistivity of porous materials such as sandstones has been investigated by many researchers [17-24], dating back as early as 1904 [17]. Fricke et al. [18] considered sandstones saturated with water as a two-component system composed of a non-conductive solid matrix and a conductive water phase.

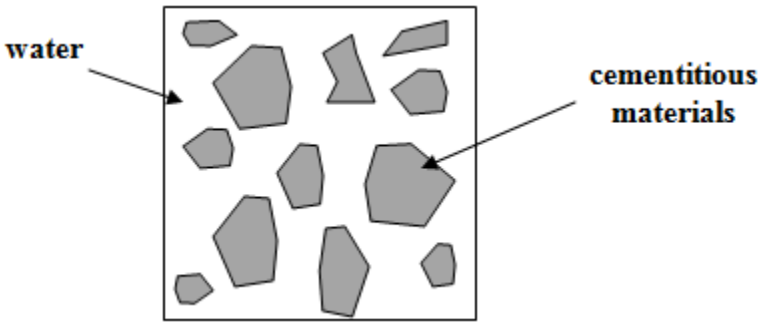

Figure 2.1 Schematic representation of cement paste structure in fresh state.

Since the electrical resistivity of solid particles is several orders larger than that of conductive water in sandstones [25], conductivity (or resistivity) of the sandstone was assumed to be mainly governed by the conductivity (or resistivity) of the water phase. A parameter, called

formation factor (F), was defined as the ratio of electrical resistivity of saturated sandstone (ρ_0) to that of water contained in its pores (ρ_w) via [17, 18, 24]:

$$F = \frac{\rho_0}{\rho_w} \tag{2.1}$$

Different empirical equations were proposed by researchers to establish a relationship between formation factor, F, and volumetric fraction of conductive component (such as water in sandstones) defined mostly in terms of porosity [17, 23, 24, 26, 27], φ. For example, Maxwell [17] proposed the formation factor (F) as a function of porosity (φ) for spherical solid particles separated in a matrix by large distances compared to their radius as:

$$F = \frac{3-\varphi}{2\varphi} \tag{2.2}$$

Similarly, Slawinski [24] derived an empirical relationship for spherical solid soil particles both in contact with each other and dispersed in the water/liquid matrix as follows:

$$F = \frac{(1.3219-0.3219\varphi)^2}{\varphi} \tag{2.3}$$

The first version of the Archie's law, which is still widely used today, was first proposed in 1942 [26] while he was studying electrical resistivity of sandstones (rocks) 100% saturated with water as follows:

$$F = \frac{\rho_0}{\rho_w} = \varphi^{-m} \tag{2.4}$$

where m is a factor that depends on the type of the porous medium. Pirson [23] suggested that exponent m ranges from 1.3 to 2.2 for slightly and highly cemented rocks, respectively. Atkins and Smith [27] improved the Archie's equation (Eq. 2.4) for rocks with multi-size particles (e.g.,

sands that are mixed with clays)by adding an empirical constant, A, to incorporate the effects of the shape and distribution of particles in the matrix via:

$$F = A\varphi^{-m} \tag{2.5}$$

where A was defined as the geometric tortuosity of a the porous material, which affects the connectivity of the pores within the matrix.

Application of Archie's law (Eq. 2.5) in cement-based materials such as concrete [9-12] and cement paste [13, 14] has been studied mainly in hardened state. It has been shown in past research that electrical properties of hardened concrete, such as its electrical resistivity or formation factor, can be used to predict durability properties of concrete [4-15]. One advantage of this approach is that electrical properties of concrete can be determined rapidly and related to other more time consuming and expensive tests such as rapid chloride penetration test (RCPT) [4-8]. Recently, methodology toward performance specifications was proposed to link electrical resistivity, RCPT and chloride transport in hardened concrete using formation factor [28].

Despite the progress in hardened concrete, formation factor in fresh state has not been investigated systematically. Specifically, the applicability of the formation factor equations proposed by other researchers for hardened porous materials (e.g. Eqs. 2.2, 2.3) have not been tested for fresh cement paste systems. For instance, as shown in Fig. 2.2, the estimated F values by Slawinski's equation (Eq. 2.3) cannot capture the actual F values obtained from experiments (F_{exp}) performed by the authors (R^2 of the data fit to the 45ºC line is less than 0.01). In addition, effects of size, shape and distribution of cementitious materials on formation factor of fresh cement paste have not been investigated. Therefore, additional studies are required to understand the variation of the formation factor in different types of fresh cement paste mixtures.

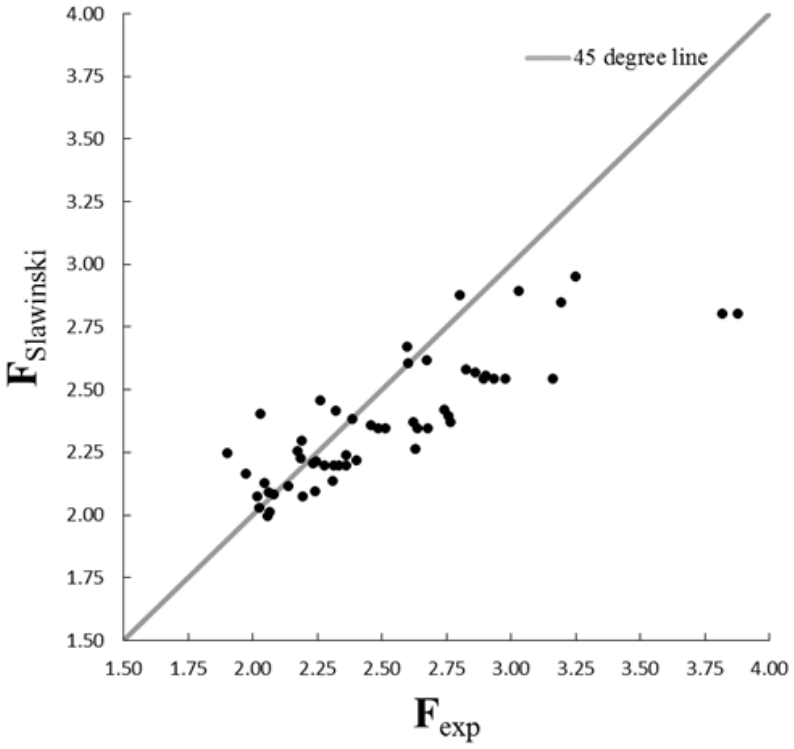

Figure 2.2 Formation factor values obtained from Eq. 2.3 (Slawinski's equation) versus experimental data. R^2 of the data fit to the 45° line, y = x, is less than 0.01.

In a cement paste mixture in fresh state, paste electrical resistivity depends on the pore solution electrical resistivity and physical formation of cementitious material particles (non-conductive component) in the solution. The former is a function of the activity of the ions released into pore solution because of chemical reactions between cementitious materials and water. The latter represents the physical configuration of solid particles and their volumetric fraction (i.e., 1-φ) in the cement paste. Therefore, in this study the Formation factor (F) for the fresh cement paste system is defined as the ratio of the electrical resistivities of the paste (ρ_p) and the pore solution (ρ_{ps}) at 25°C via:

$$F = \frac{\rho_p}{\rho_{ps}} \tag{2.6}$$

Chapter 3 Method

3.1 Materials

Cement paste mixtures were prepared by mixing cementitious materials (cm) and distilled water (w) in different ratios. The conductivity of the mixing water was 42.5 □S/cm, indicating very low ionic contamination. Type I OPC and blended cements with low, medium and high mass replacement of SCMs (i.e., fly ash, silica fume and slag) were used as cementitious materials. Mass replacement levels of blended systems were 10%, 30%, and 50% for fly ash and slag, and 5%, 10%, and 15% for silica fume. The chemical and physical properties of these cementitious materials are presented in Table 3.1.

Table 3.1 Chemical and physical properties of cementitious materials.

	OPC (% of mass)	**Silica Fume** (% of mass)	**Fly Ash** (% of mass)	**Slag** (% of mass)
Na_2O	0.08	0.08	0.94	0.30
MgO	3.23	0.47	1.28	10.09
Al_2O_3	4.74	0.19	18.37	7.95
SiO_2	19.74	93.50	36.56	37.84
P_2O_5	0.06	0.11	0.13	0.01
SO_3	3.06	0.04	0.63	0.48
K_2O	0.56	0.92	1.78	0.42
CaO	63.68	0.30	3.56	39.09
TiO_2	0.26	0.02	0.80	0.79
MnO	0.04	0.11	0.23	0.47
Fe_2O_3	1.8	1.56	32.47	0.47
Particle density(g/cm^3)	3.14	2.30	2.70	2.90
Fineness(cm^2/g)	3555	195000	4500	5970
Average size (μm)	10	0.1	15	45

Some of the mixtures included a polycarboxilate-based superplasticizer (BASF MasterGlenium 3030), which was added to distilled water in three dosages: 0.2%, 0.5%, and 1.0% (by mass). The density of superplasticizer was reported by the manufacturer to be close to that of water at 25 °C (i.e., 1 g/cm^3), and its conductivity was 5.42 mS/cm. Since the dosage of the superplasticizer was less than 1.0% (by mass) of the liquid phase, the conductivity of the mixing water after adding the superplasticizer was relatively low (102.7 □S/cm for 1.0% dosage) assuring that the ionic contamination in the mix water due to the use of superplasticizer was not significant.

3.2 Sample Preparation

Five types of cement paste mixtures were prepared in this study: (1) OPC, (2) OPC plus superplasticizer, (3) OPC plus fly ash, (4) OPC plus silica fume, and (5) OPC plus slag. In total, 54 different paste samples were prepared and tested. In addition, 17 replica pastes were made to test the reproducibility of the data obtained from the experiments. The water-to-cementitious-material ratio, w/cm, of the mixtures ranged from 0.3 to 0.55 with 0.05 increments to cover a wide range of possible w/cm used in the construction industry. In Tables 3.2 to 3.6, the detailed proportions of all 54 cement paste mixtures used in this study are presented. In these tables and the paper, superplasticizer, fly ash, silica fume, and slag are denoted by SP, FA, SF, and SL, respectively. In the labeling convention, the w/cm and the SCM (or superplasticizer) replacement levels are designated; for instance, “P0.45-SF15” identifies a paste with a w/cm of 0.45 containing 15% (mass) of silica fume (i.e., 85% by mass OPC). The exact times of adding water to the cementitious materials, and subsequent mixing time, were recorded. Blending of mixture continued until homogeneous paste was obtained after about 4 minutes. The fixed volume of

paste was then poured into a cylindrical mold with 75.0 mm diameter in a way that the height of fresh paste in the mold was 50.0 ±1.0 mm for all of the mixtures.

Table 3.2 Mixture proportion of the OPC pastes.

Paste ID	w/cm	OPC (g)	W (g)	SCM/SP (%)	SP (g)	FA (g)	SL (g)	SF (g)
P0.35	0.35	800	280	0	0	0	0	0
P0.4	0.4	700	280	0	0	0	0	0
P0.45	0.45	600	270	0	0	0	0	0
P0.5	0.5	500	250	0	0	0	0	0

Table 3.3 Mixture proportion of the OPC pastes with superplasticizer.

Paste ID	w/cm	OPC (g)	W (g)	SCM/SP (%)	SP (g)	FA (g)	SL (g)	SF (g)
P0.35-SP0.2	0.35	800	278.4	0.2	1.6	0	0	0
P0.4-SP0.2	0.4	700	278.6	0.2	1.4	0	0	0
P0.45-SP0.2	0.45	600	268.8	0.2	1.2	0	0	0
P0.5-SP0.2	0.5	500	249	0.2	1	0	0	0
P0.3-SP0.5	0.3	800	236	0.5	4	0	0	0
P0.35-SP0.5	0.35	750	258.75	0.5	3.75	0	0	0
P0.4-SP0.5	0.4	700	276.5	0.5	3.5	0	0	0
P0.45-SP0.5	0.45	600	267	0.5	3	0	0	0
P0.3-SP1.0	0.3	800	232	1	8	0	0	0
P0.35-SP1.0	0.35	750	255	1	7.5	0	0	0
P0.4-SP1.0	0.4	700	273	1	7	0	0	0
P0.45-SP1.0	0.45	600	264	1	6	0	0	0

Table 3.4 Mixture proportions of the OPC pastes with fly ash.

Paste ID	w/cm	OPC (g)	W (g)	SCM/SP (%)	SP (g)	FA (g)	SL (g)	SF (g)
P0.35-FA10	0.35	720	280	10	0	80	0	0
P0.4-FA10	0.4	675	300	10	0	75	0	0
P0.45-FA10	0.45	630	315	10	0	70	0	0
P0.5-FA10	0.5	540	300	10	0	60	0	0
P0.35-FA30	0.3	560	240	30	0	240	0	0
P0.35-FA30	0.35	525	262.5	30	0	225	0	0
P0.4-FA30	0.4	490	280	30	0	210	0	0
P0.45-FA30	0.45	420	270	30	0	180	0	0
P0.5-FA30	0.5	420	300	30	0	180	0	0
P0.35-FA50	0.3	400	240	50	0	400	0	0
P0.35-FA50	0.35	375	262.5	50	0	375	0	0
P0.4-FA50	0.4	350	280	50	0	350	0	0
P0.45-FA50	0.45	300	270	50	0	300	0	0
P0.5-FA50	0.5	300	300	50	0	300	0	0

Table 3.5 Detailed mixture proportion of the OPC pastes with silica fume.

Paste ID	w/cm	OPC (g)	W (g)	SCM/SP (%)	SP (g)	FA (g)	SL (g)	SF (g)
P0.4-SF5	0.4	760	320	5	0	0	0	40
P0.45-SF5	0.45	712.5	337.5	5	0	0	0	37.5
P0.5-SF5	0.5	665	350	5	0	0	0	35
P0.55-SF5	0.55	570	330	5	0	0	0	30
P0.4-SF10	0.4	720	320	10	0	0	0	80
P0.45-SF10	0.45	675	337.5	10	0	0	0	75
P0.5-SF10	0.5	630	350	10	0	0	0	70
P0.55-SF10	0.55	540	330	10	0	0	0	60
P0.4-SF15	0.4	680	320	15	0	0	0	120
P0.45-SF15	0.45	637.5	337.5	15	0	0	0	112.5
P0.5-SF15	0.5	595	350	15	0	0	0	105
P0.55-SF15	0.55	510	330	15	0	0	0	90

Table 3.6 Detailed mixture proportion of the OPC pastes with slag.

Paste ID	w/cm	OPC (g)	W (g)	SCM/SP (%)	SP (g)	FA (g)	SL (g)	SF (g)
P0.35-SL10	0.35	720	280	10	0	0	80	0
P0.4-SL10	0.4	675	300	10	0	0	75	0
P0.45-SL10	0.45	630	315	10	0	0	70	0
P0.5-SL10	0.5	540	300	10	0	0	60	0
P0.3-SL30	0.3	560	240	30	0	0	240	0
P0.35-SL30	0.35	525	262.5	30	0	0	225	0
P0.4-SL30	0.4	490	280	30	0	0	210	0
P0.45-SL30	0.45	420	270	30	0	0	180	0
P0.3-SL50	0.3	400	240	50	0	0	400	0
P0.35-SL50	0.35	375	262.5	50	0	0	375	0
P0.4-SL50	0.4	350	280	50	0	0	350	0
P0.45-SL50	0.45	300	270	50	0	0	300	0

3.3 Electrical Resistivity Measurements

3.3.1 Paste

Electrical resistivity of fresh paste was monitored during the first 2 hours after mixing. AC impedance spectroscopy (using Giatec RCON^{TM} [29]) was employed to obtain resistivity of fresh pastes. The schematic illustration of the test setup is given in Fig. 3.1. A constant AC current of 10 μA was applied through two electrodes and corresponding impedance was recorded. The internal temperature of paste was also recorded to consider temperature change due to heat release as a result of hydration of OPC and pozzolanic reactions of SCMs. The equation, which was shown to be applicable to fresh concrete, mortars and cement paste [12, 30-34], was used to normalize the resistivity values to a reference temperature of 25 °C:

$$\rho_\theta = \left(1+\alpha(T-\theta)\right)\rho_T \tag{3.1}$$

where ρ_T and ρ_θ are resistivities of concrete at T (°C) and θ(°C), respectively; and α ($°C^{-1}$) is the temperature coefficient of resistivity. In this study, α was experimentally obtained to be 0.013 $°C^{-1}$.

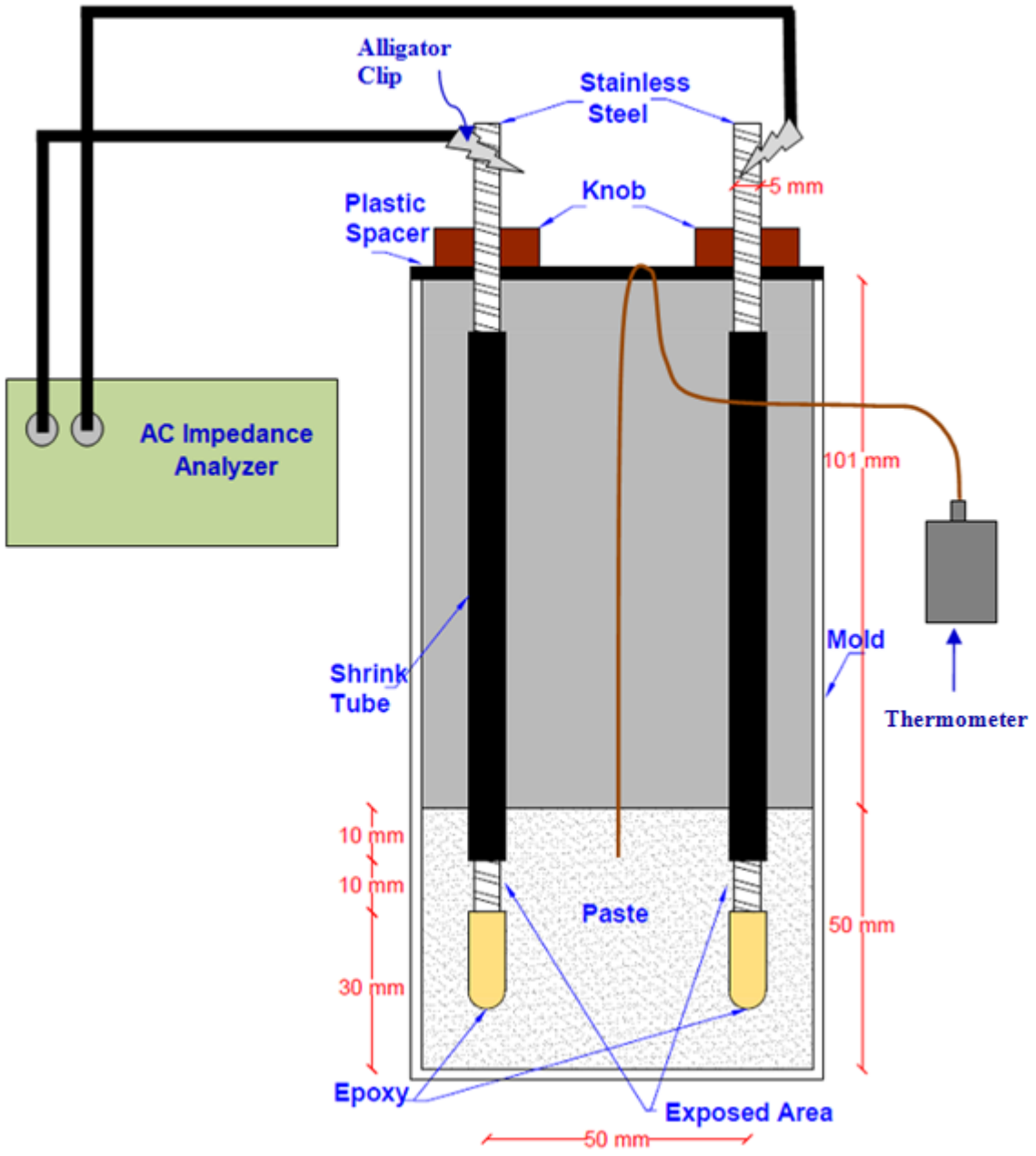

Figure 3.1 Schematic illustration of the test setup for electrical resistivity measurements.

The electrical resistivity of a cement paste (ρ_p) can be obtained from its measured electrical impedance. Electrical impedance of paste is equal to its resistance (R_p) when phase angle between current and potential approaches zero. The electrical resistivity of paste can then be calculated by calibrating the apparatus with an ionic solution of known conductivity and applying equation:

$$\rho_p = \frac{R_p}{R_{ref}} \rho_{ref} \tag{3.2}$$

where ρ_p is the electrical resistivity of the paste (Ω-m); ρ_{ref} is the known electrical resistivity of the reference solution (Ω-m); R_p is the measured electrical impedance of the specimen (Ω); and R_{ref} is the measured electrical impedance of the reference solution in the specimen holder (mold) (Ω).

3.3.2 Pore Solution

Direct measurement of pore solution resistivity/conductivity requires the extraction of pore solution from the fresh paste. In this study the extraction process was conducted at the 30th, 60th and 90th minute after mixing the materials. The liquid phase of the fresh paste (i.e., pore solution) can be separated out with different methods such as using a centrifuge or vacuum pump. In this research, a GAST vacuum pump with a maximum vacuum pressure of 760 mmHg was used to apply suction. The pressure during the extraction process was constant 600 mmHg. Also, an Erlenmeyer flask with a side port, a funnel, sealing rubber and 3 layers of Whatman™ filter papers with pore size of 20-25 μm (i.e., one larger with 185 mm diameter to cover the entire internal wall of funnel and confine the paste sample, and two smaller 50 mm diameter at the bottom of the funnel to avoid tearing up as a result of stress concentration at that point) were used in the setup shown in Fig. 3.2 to perform the extraction process.

(a)

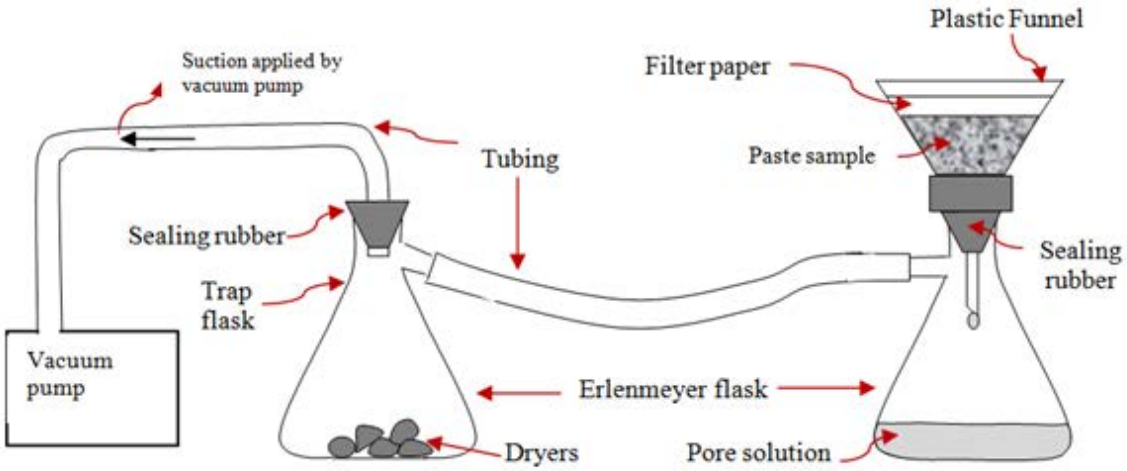

(b)

Figure 3.2 Test setup to apply suction through vacuum pump for pore solution extraction: a) actual experimental setup; b) schematic diagram.

The suction/extraction process was around 6 minutes on average for collecting about 20 ml of pore solution, but highly depended on the w/cm of the paste samples. The pore solutions were stored in plastic tubes (with little to no top air space) with air-tight lids to prevent

carbonation and other forms of contamination. A conductivity meter, SymPHony SP90M5, was used to measure conductivity of pore solution samples. It had a temperature sensor and was set to directly give the conductivity at a reference temperature of 25°C.

3.3.3 Selection of Effective Frequency

AC impedance analyzer measures the impedance, rather than the electrical resistance, of the paste sample between the two electrodes as shown in Fig. 3.1. In order to convert the impedance measurements to resistance, the capacitance effect should be eliminated, which occurs when the phase angle between the signals of applied current and recorded voltage of AC impedance analyzer becomes zero, as in the case of a pure resistor. In order to determine the resistance of a fresh paste, a preliminary study was conducted to determine the effective frequency corresponding to the lowest phase angle (i.e., closest to zero). In this study, the frequency of the measurements was swept from 1 to 30,000 Hz to obtain the impedance spectrum of the cement paste system (Figure 3.3). Fig 3.3 shows the variation of impedance and phase angle with frequency in a typical paste mixture (OPC, w/c=0.45). Each sweeping cycle took around 3 minutes. The impedance spectra were recorded during the first two hours after mixing the materials. Fig. 3.3 indicates that the rate of change in impedance after 1,000 Hz is negligible. In addition, the phase angle decreases with increasing the frequency up to 10 kHz and then it becomes stable. Therefore, the frequency of 30 kHz was chosen in this study to measure the electrical resistivity of fresh pastes. At this frequency, the phase angle of the measurements (values on secondary vertical axis) was around 4 degrees.

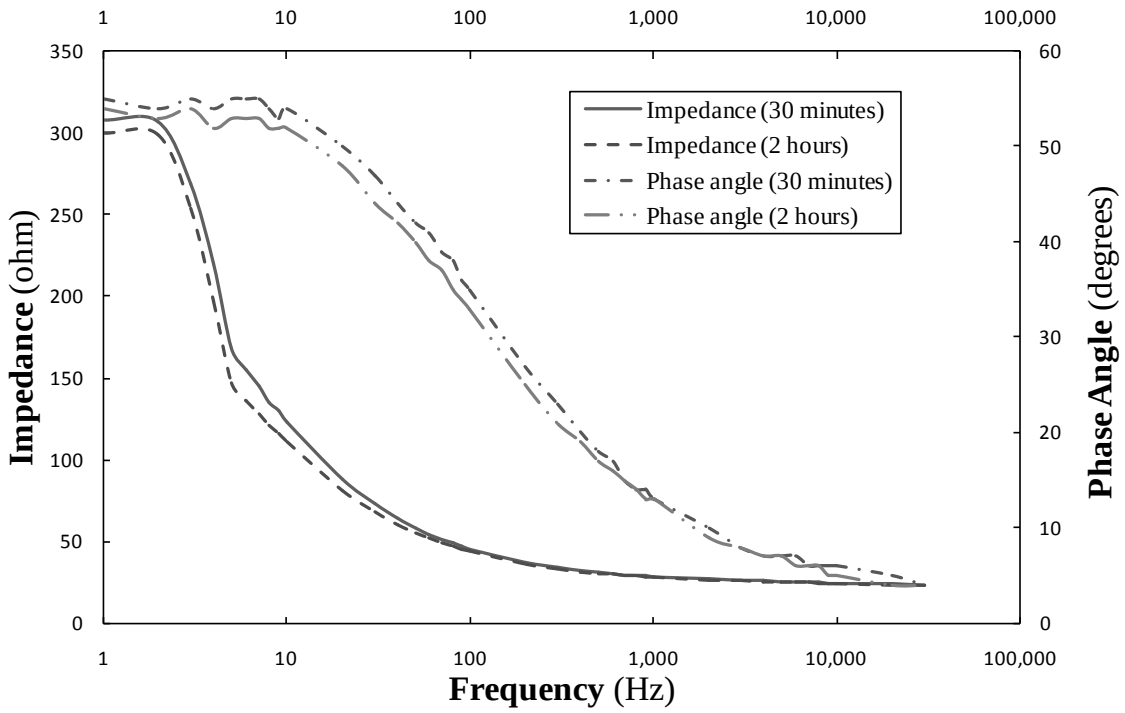

Figure 3.3 Measured impedance and phase angle in one cycle of frequency sweep. Although measurements were taken at different times of fresh state, for clarity, data from only two sweeps (at 30 minutes and 2 hours) are shown.

Chapter 4 Results and Discussion

4.1 Formation factor variation with time

To explore the effect of paste age (i.e., time) on formation factor during the fresh state, a paste with w/cm ratio of 0.45 was selected in our study because w/cm ratio of 0.45 resulted in the most homogenous and non-segregated paste. Furthermore, medium dosage mass replacement (MR) of SCMs in cementitious materials as well as superplasticizer was selected for each type of paste mixture. The average results of paste and pore solution resistivity from repetitive tests at 30^{th}, 60^{th}, and 90^{th} minute of paste age are shown in Fig. 4.1; and the error bars with one standard deviation are also plotted on the curves. Using Eq. 6, the formation factor values were then calculated which are shown in Fig. 4.2.

Figure 4.2 shows that for each type of paste mixture (e.g. P0.45-SP0.5) during fresh state, the formation factor does not change significantly over time considering the errors associated with each data. Therefore, although both paste and pore solution resistivity decrease with time (see Fig. 4.1) during fresh state [35, 36], the ratio of electrical resistivity of the paste to pore solution, i.e., formation factor, does not vary during fresh state and is almost constant. As discussed earlier, the formation factor indicates the physical formation of the paste; i.e., fraction of solid particles in the paste mixture, their shape, size and distribution in the pore solution. Since in a given paste mixture with a constant w/cm ratio determined in the mixture design, the type of cementitious materials (i.e., solid particles) does not change over time, the fraction of solid particles in the paste, their shape, size and distributions do not also vary over time during fresh state. However, the formation factor varied when the SCMs or superplasticizer were added to the mixture (Fig. 4.2) as these additives would change the fraction of solid particles, their shape, size and distributions in the paste .

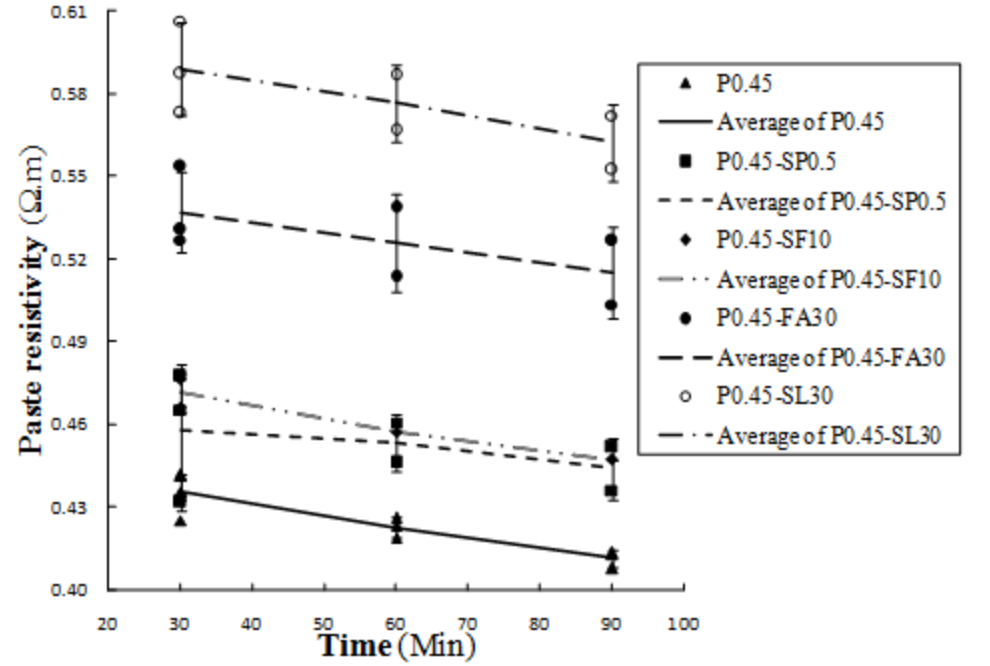

(a)

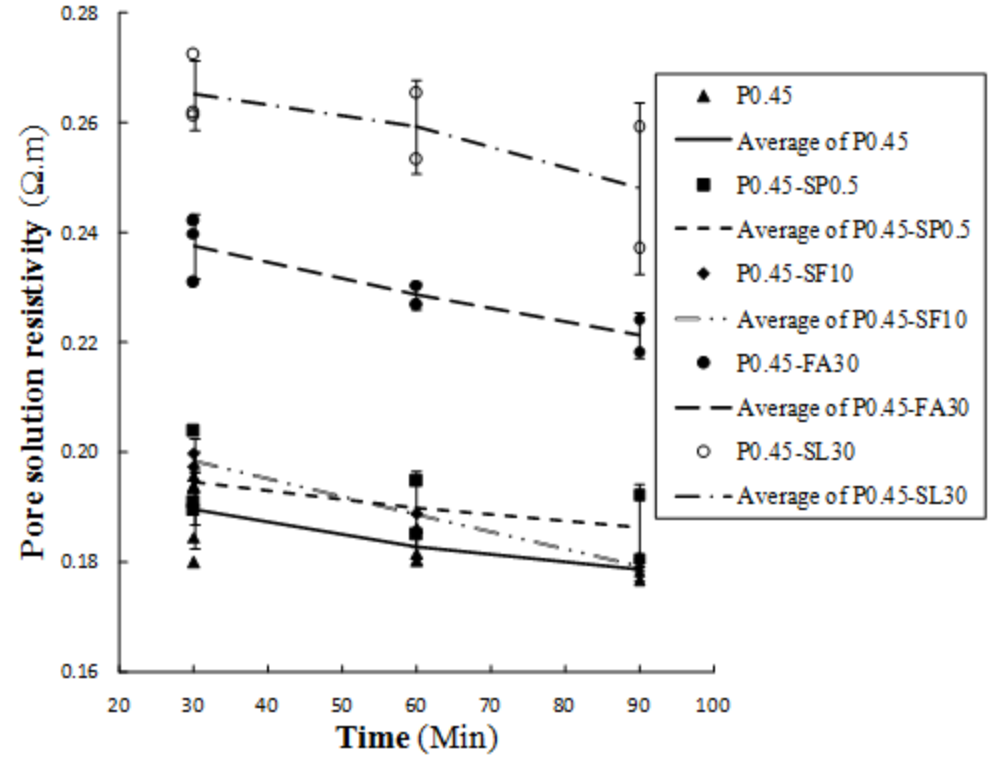

(b)

Figure 4.1 Resistivity variation with time for the paste mixtures with w/cm ratio of 0.45 during fresh state: a) paste electrical resistivity; b) pore solution electrical resistivity.

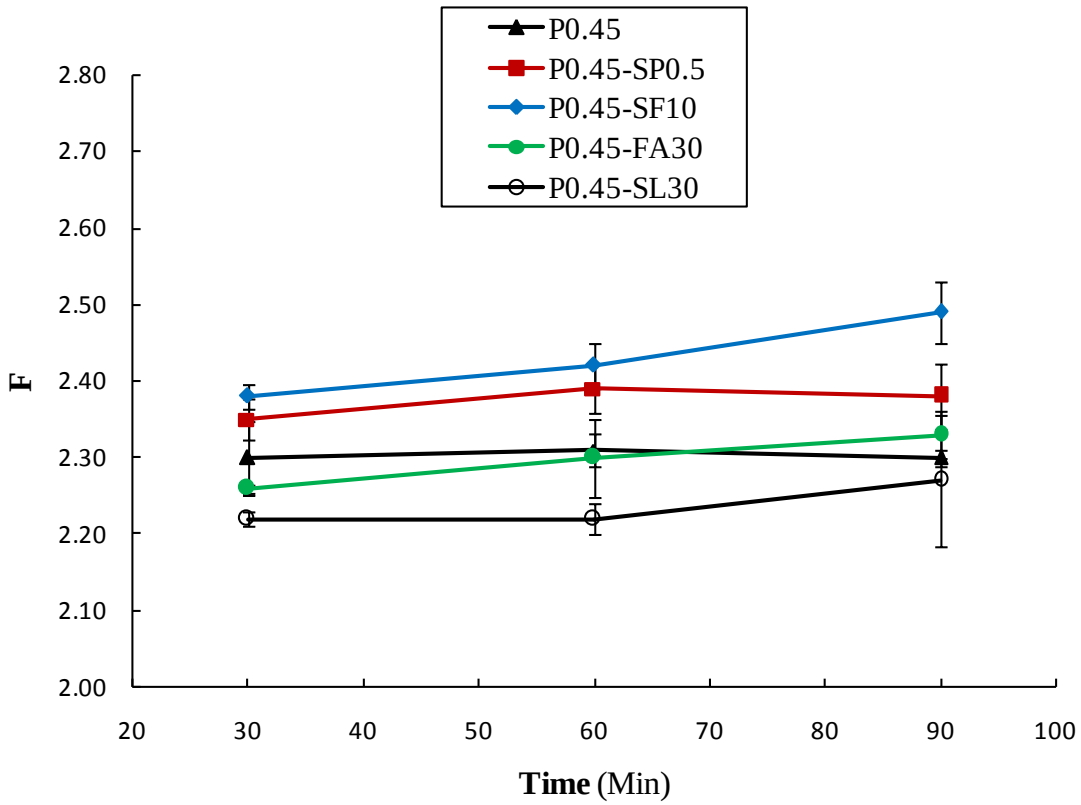

Figure 4.2 Formation factor versus time after mixing the cement paste (age) for mixtures with w/cm of 0.45 and medium dosage replacement of SCMs or superplasticizer.

Most importantly, the stable behavior of formation factor revealed that no significant amount of hydration products such as C-S-H formed during fresh state (around 2 hours for w/cm of 0.45) before setting time of the cementitious materials. It is expected that at the initial setting time of paste mixture, which is onset of solidification, the formation factor starts to rise sharply. Fig. 4.3(a) schematically shows the initial setting time (t_i) point determined on an F-Time curve. The extracted data from Sant et al. [36] research in Fig. 4.3(b) is an example which shows the sharp increase in formation factor around 100 minutes after mixing the materials. Therefore, monitoring the formation factor development with time can be used as an effective tool to determine the initial setting of cement-based materials which has always been a challenge [9, 37]

given that traditional Vicat penetration method [38] is time-consuming and fairly dependent on technician's skill.

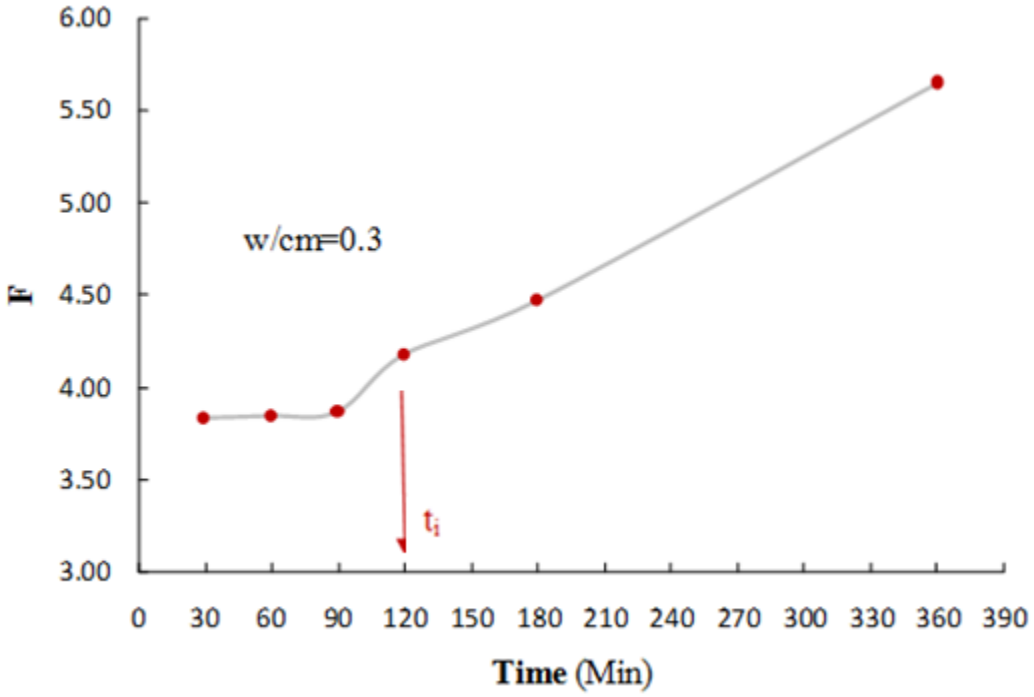

Figure 4.3 Determination of initial setting time (t_i) of cement-based materials on Formation factor-Time curve: applicability of the method in a cement paste mixture with w/cm of 0.3 [35].

4.2 Formation factor versus porosity

Porosity is defined as volumetric fraction of liquid phase (water plus superplasticizer) in the paste mixture, whereas w/cm ratio is the weighted ratio of liquid phase (w) to total cementitious materials (cm). Accordingly, porosity φ can be expressed as follows:

$$\varphi = \frac{V_w}{V_w + V_{cm}} = \frac{V_w}{V_w + V_{OPC} + V_{SCM}} \quad (4.1)$$

where V_w, V_{OPC}, and V_{SCM} are the volume of the liquid phase, ordinary portland cement, and supplementary cementitious material, respectively. The density of water and superplasticizer at 25 °C were reported as 1.00 g/cm^3. Given the density of the cementitious materials at 25°C and SCMs replacement, Eq. 4.1 can be rewritten as:

$$\varphi = \frac{w/cm}{w/cm + \frac{(1-MR)}{D_{OPC}} + \frac{MR}{D_{SCM}}} \tag{4.2}$$

$$\frac{1}{\varphi} = 1 + \frac{\frac{(1-MR)}{D_{OPC}} + \frac{MR}{D_{SCM}}}{w/cm} \tag{4.3}$$

where D_{OPC} and D_{SCM} are the particle density of OPC and supplementary cementitious material (see Table 3.1), respectively; and MR is the SCM mass replacement ratio to the total cementitious materials; e.g. MR is 0.1 for 10% silica fume incorporated paste mixture. Eq. 4.3 which is obtained by inversing both sides of Eq. 4.2 exhibits that porosity and w/cm ratio are directly proportional when D_{SCM} and MR are constants; i.e., the greater the designated w/cm, the higher the paste porosity for a particular paste mixture.

If a fresh paste is modeled as a circuit with two parallel resistors (pore solution resistance, R_{ps}, and solid cementitious particle resistance, R_s), the resistance of paste (R_p) as equivalent resistance of the electrical circuit can be expressed via:

$$R_p = \frac{R_s \times R_{ps}}{R_s + R_{ps}} \tag{4.4}$$

Since resistance of solid particles are several orders higher than that of pore solution (i.e., $R_{ps}/R_s \rightarrow 0$), dividing numerator and denominator of Eq. 4.4 by R_s, R_p can be approximated as:

$$R_P \approx R_{PS} \tag{4.5}$$

Equation 4.5 indicates that in a simplified two-parallel-resistor model, all electrical charge transfer occurs in pore solution. Defining Eq. 4.5 in terms of resistivity, considering the geometry of parallel resistor model, results in:

$$\frac{\rho_p \times L_p}{A_p} = \frac{\rho_{ps} \times L_{ps}}{A_{ps}} \tag{4.6}$$

where L_p and L_{ps} are the average lengths of electrical charge pathways for the paste and pore solution, respectively; and A_p and A_{ps} are the sectional areas of the paste and pore solution, respectively. Therefore, considering the definition of porosity in Fig. 2.1 (i.e., $A_{ps}/A_p=\varphi$) and tortuosity (i.e., the relative length of electrical charge transfer pathway), Eq. 4.6 can be rewritten as follows:

$$F = \frac{\rho_P}{\rho_{PS}} = (\frac{L_{PS}}{L_P})(\frac{A_P}{A_{PS}}) \quad (4.7)$$

For each type of paste mixture in this study including OPC pastes with or without SCMs (e.g. silica fume, fly ash, slag) and superplasticizer, the electrical resistivity of the paste and associated pore solution at 30th min after mixing the materials at the reference temperature of 25 °C were obtained. The formation factors were then calculated. Although the measurements were conducted at 30th minute, based on the discussion made in the last section, formation factor results are almost equal at any time during the fresh state.

To investigate applicability of the Archie's law in fresh cement paste mixture, variation of formation factor with porosity was plotted for each type of paste mixture including OPC pastes incorporated with silica fume, fly ash, slag and superplasticizer. The results are shown in Fig. 4.4.

The graphs in Fig. 4.4 indicate that the relationship between formation factor of fresh cement paste and its porosity can be (i.e., R^2 values are quite high and close to 1) defined using Archie's law (i.e., power function). By using a power regression analysis, the associated parameters A and m of Archie's equation were found for each type of paste mixture and presented in Table 4.1; e.g. A and m for OPC paste mixture are 0.847 and 1.93, respectively. From purely mathematical viewpoint, the m which is called shape factor indicates the sensitivity of formation factor to variation in porosity (the slope of the curve); i.e., the higher the m value of

a paste mixture, the more drop in formation factor value per unit increase in porosity. However, the experimental constant A (i.e., tortuosity) is more representative of magnitude of formation factor in general and will be discussed in detail later.

In addition, in Fig. 4.5, all the obtained formation factor (F) data for various mixtures were plotted to evaluate whether a unified simple equation can be used for all types of cement paste mixtures in this study with a reasonable accuracy. R^2 value of 0.845 indicated that even by considering one equation for all types of the mixtures, rather good correlation still exists between the formation factor and porosity even though with less correlativity.

Table 4.1 Parameters of Archie's law obtained from regression analysis for each type of paste mixture.

Paste mixture	A	m	R^2
OPC	0.847	1.93	0.99
OPC+SP0.2	0.497	2.86	1.00
OPC+SP0.5	0.490	2.81	0.97
OPC+SP1.0	0.523	2.71	0.98
OPC+FA10	0.695	2.18	0.98
OPC+FA30	0.848	1.69	0.99
OPC+FA50	0.689	1.98	0.97
OPC+SF5	0.736	2.21	0.99
OPC+SF10	0.700	2.25	0.96
OPC+SF15	0.695	2.30	0.93
OPC+SL10	0.710	2.14	0.99
OPC+SL30	0.713	2.05	0.99
OPC+SL50	0.568	2.18	0.93

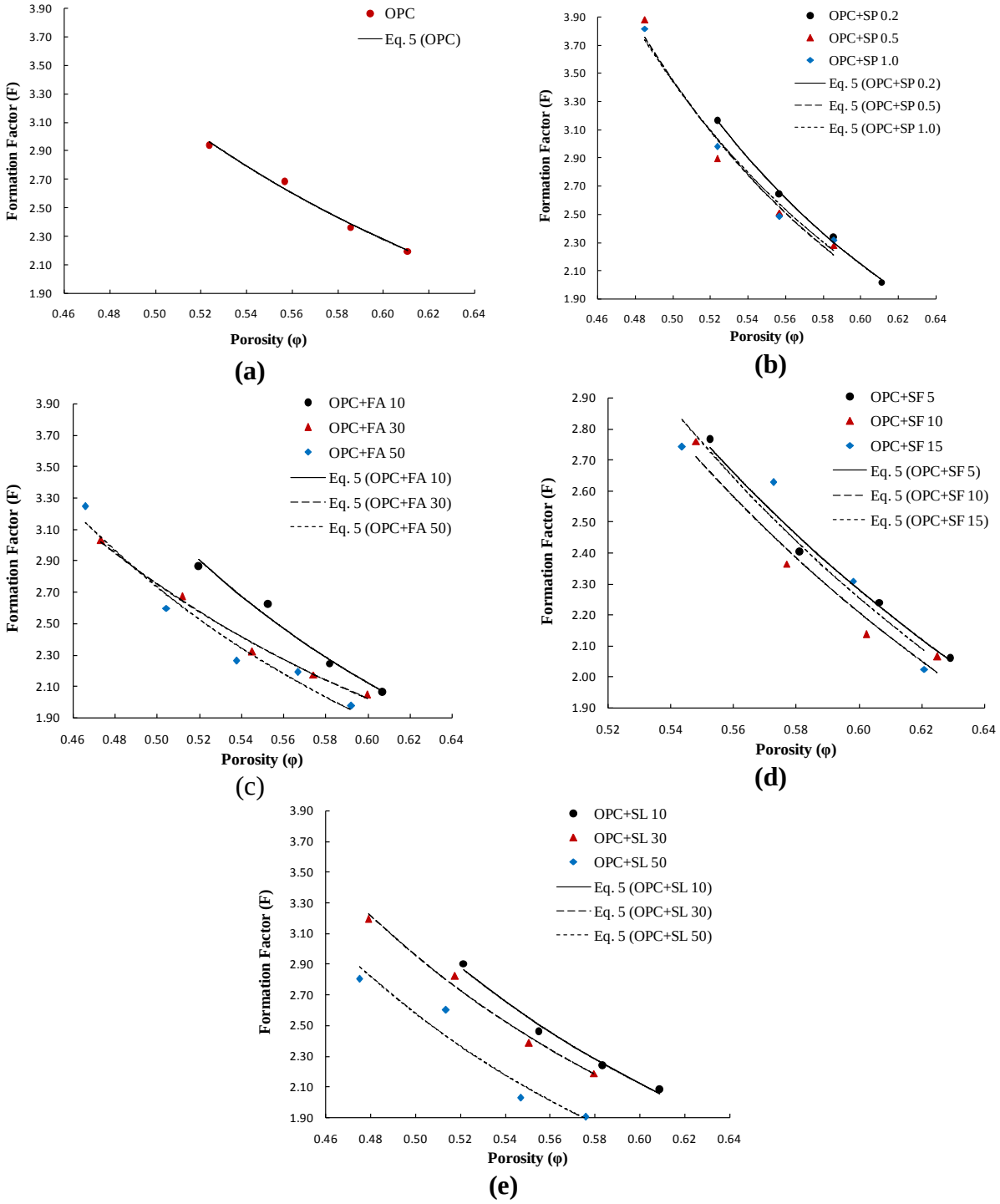

Figure 4.4 Formation factor versus porosity of fresh cement pastes: a) OPC; b) OPC plus superplasticizer; c) OPC plus fly ash; d) OPC plus silica fume ; e) OPC plus slag.

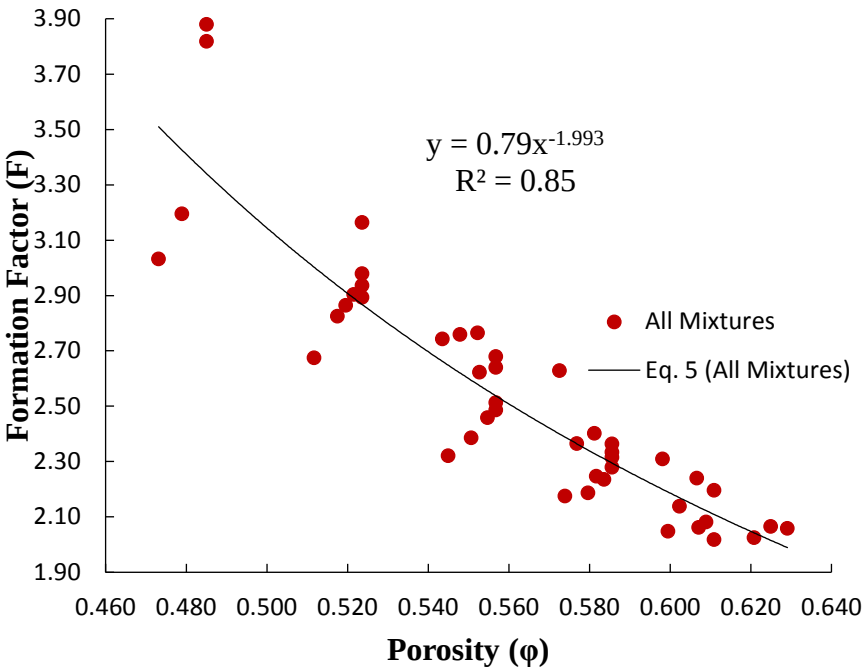

Figure 4.5 Formation factor versus porosity of fresh OPC paste with or without superplasticizer, silica fume, fly ash and slag.

4.3 Tortuosity

As schematically shown in Fig. 4.6, tortuosity of a paste mixture qualitatively indicates the average length of electrical charge transfer pathways in the pore solution which depends on the distribution, size and shape of the cementitious material particles. Therefore, higher tortuosity shows that ions in the pore solution must take more convoluted pathways due to the presence of solid particles. All the mentioned effects on the movement of ions through solid particles can be schematically seen in Fig. 4.6. It shows that even for a same porosity (i.e., the shades area is fixed in all figures of a, b, c and d), better distributed, smaller, and more angular solid cementitious particles result in higher tortuosity (longer pathway for ions/charge transport).

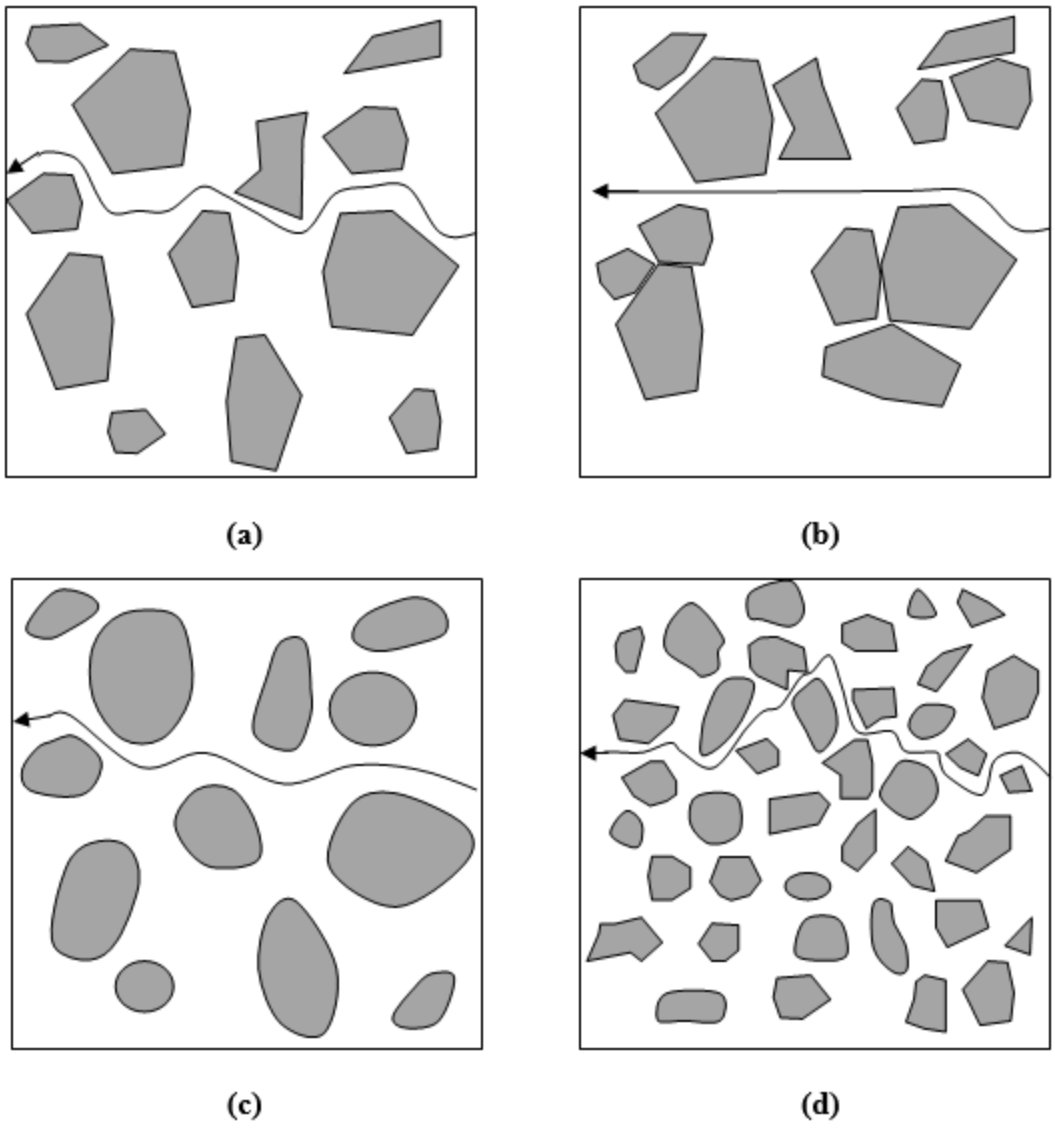

Figure 4.6 Schematic of charge transfer in the pore solution and the solid cementitious particles with the same porosity: a) normal distribution of particles; b) aggregated particles; c) round shape particles; and d) small size particles.

The tortuosity of a paste mixture can be experimentally quantified using Archie's law through the coefficient A and the formation factor-porosity curves such as those shown in Fig. 4.4. However, using the regression analysis to compare the tortuosity values of different types of paste mixtures requires to set a constant m as a reference for all of them to eliminate the effect

of porosity variation on formation factor; i.e., when two different paste mixtures have the same porosity, formation factor difference between them is purely affected by their tortuosity.

The reference m for our analysis was selected from the curve which gave the best agreement with data from all different types of paste mixtures used in our study. The trend line in Fig. 4.5 shows that 1.99 was the most suitable value and thus was chosen as our reference m to find tortuosity. To find the corresponding coefficient A using the value of 1.99 for m, $\varphi^{-1.99}$ was replaced by φ' to obtain a linear equation:

$$F = A\varphi^{-1.99} = A\varphi' \tag{16}$$

Using the linear regression analysis while setting intercept to 0, the tangent of linear trend line provided the coefficient A of each paste mixture.

The typical illustration of this analysis to calculate tortuosity for OPC paste is shown in Fig. 4.7, which yielded a coefficient A of 0.820. The results of such analysis to find the coefficients of all various paste mixtures in this study are shown in Fig. 13.

Fig. 4.8 shows the variation of tortuosity values for different paste mixtures indicating the complexity of electrical conduction in pore solution in the presence of various cementitious materials (solid phase). In other words, the greater the tortuosity value is, the more complex pathway for electrical charge to pass among the solid particles would be, which depends on the size, roundness and distribution of particles in the pore solution.

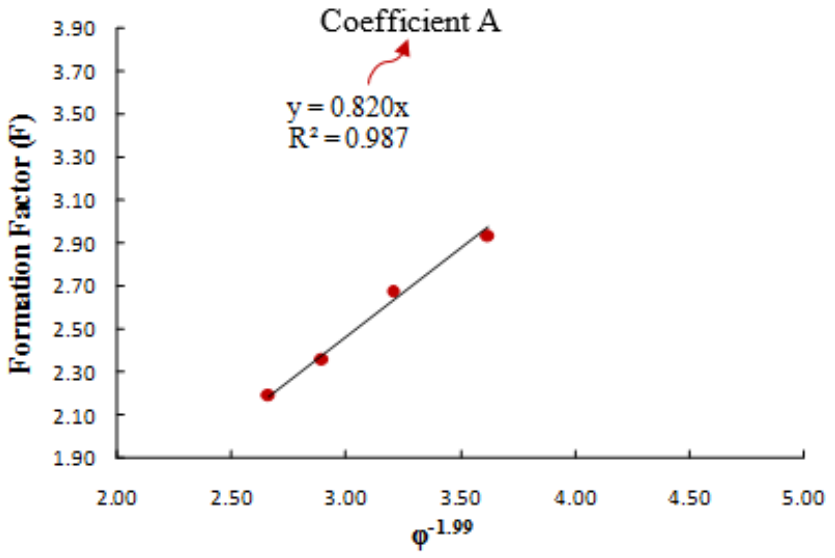

Figure 4.7 Finding tortuosity coefficient of OPC paste from formation factor (F) and porosity (φ) data using linear regression analysis.

The OPC particles have the average size around 10 μm (see Table 3.1) and they are rather spherical. Although the amount of superplasticizer dosage is relatively small (around 1/1000th of the cement mass), the data in Fig. 4.8 indicates that it increases the tortuosity value of the paste. The increase in tortuosity is attributed to the distribution effect of superplasticizer on cement particles. The cement particles naturally have a tendency to aggregate while mixing with water due to electrostatic charge and thus always a small portion of them sticks together. However, superplasticizer physically separates them by yielding electrostatic repulsion when absorbed to the cement particles. Consequently, a more complex pathway for charge transfer is made due to the better distribution of cement particles in water, which results in higher tortuosity.

Fig. 4.8 illustrates that fly ash considerably reduced the tortuosity of the paste at fresh state. The average size of fly ash particles used in this study was about 15 μm that was a bit larger than cement particles (10 μm) which resulted in less tortuosity, because less number of fly

ash particles was involved in the movement of ions compared to the cement particles. Furthermore, the considerable reduction of tortuosity in fly ash-incorporated pastes can be also related to the spherical shape of its particles (roundness); i.e., for two particles with the same size, the one that has more angular/broken shape yields a higher tortuosity.

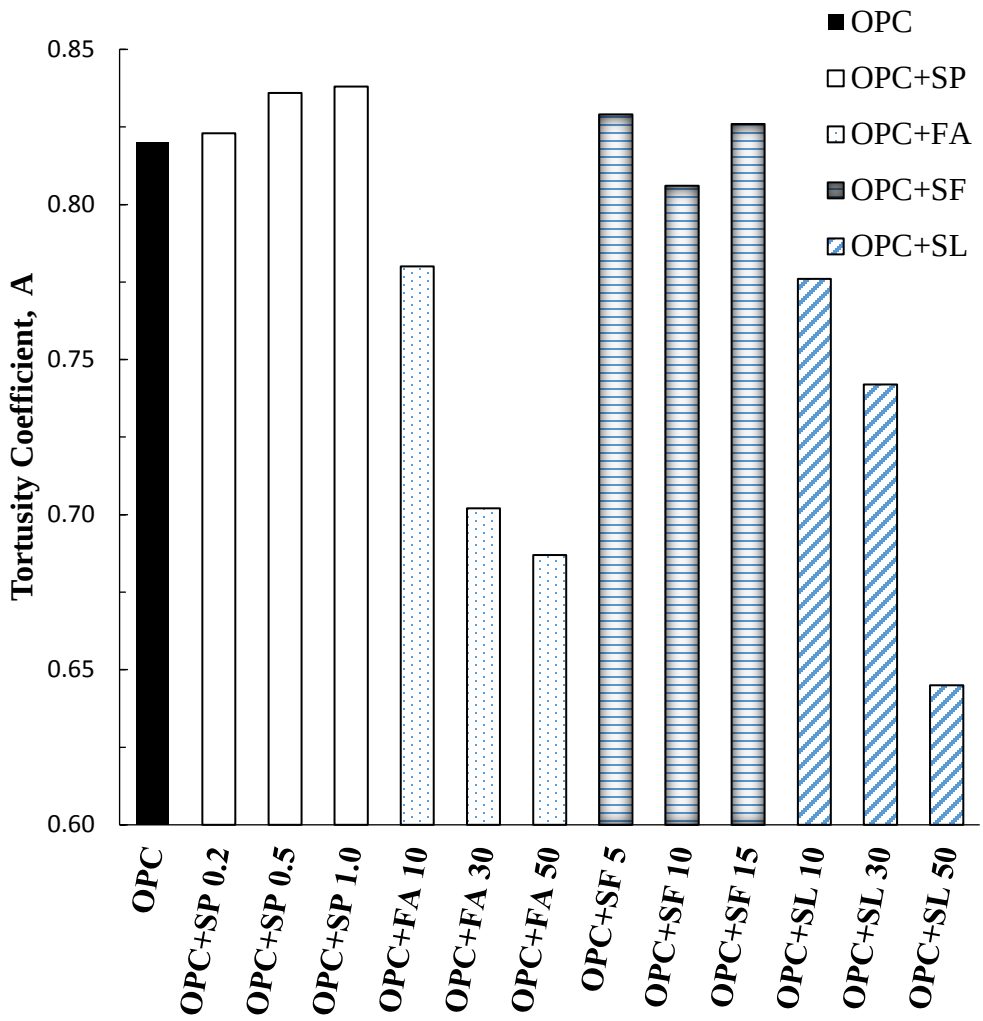

Figure 4.8 Tortuosity coefficient of various paste mixtures at fresh state.

Silica fume particles average size is around 0.1 μm which is in the order of 1/100th of the cement particles. They naturally have tendency to aggregate and are more rounded than cement particles. The former effect tends to increase the tortuosity, while the latter effect decreases the

tortuosity. Figure 4.8 shows that these two opposing effects compensated each other in a way that the resultant tortuosity from the addition of silica fume did not change significantly compared to that of the OPC mixture and had no trend with increase in silica fume dosage. Although it was expected because of very small size of silica fume particles, tortuosity increased, the roundness and aggregation effect decreased the tortuosity and none of these influential factors was dominant.

Fig. 4.8 shows that the addition of slag to the paste resulted in a large reduction in the tortuosity values. The average particle size of slag is around 45 μm, which is approximately 5 times larger than cement particles. Therefore, the number of slag particles per unit volume of the paste is about 1/25 times less than that of the cement particles. As a result, the length of ion movement pathways decreased and consequently, the tortuosity significantly decreased in the slag incorporated pastes at the fresh state. Although the roundness of slag is less than the cement particles because of sudden cooling procedure in their production, this effect was not dominant and the tortuosity value was governed by quite larger size of slag particles. The more the slag particles present in the paste mixture, the less the corresponding tortuosity would be.

Chapter 5 Conclusions and Recommendations

The main conclusions from this study can be highlighted as follows:

- For a given type of paste mixture (e.g. OPC plus silica fume), formation factor decreases if porosity or w/cm ratio increases, and this relationship can be well formulized by a power function.

- Although both paste and pore solution resistivity decrease with time in fresh cement paste mixtures until initial setting, their ratio (formation factor) remains relatively constant because it is only indicative of physical formation of solid particles in the pore solution.

- Formation factor of fresh cement paste is strongly correlated to its porosity through Archie's law, which implies that formation factor decreases if porosity increases. This decrease of formation factor is attributed to the smaller solid particles fraction (i.e., 1-φ) with high resistivity (i.e., lower amount of non-conductive component compared to conductive component).

- The tortuosity of paste affects the formation factor even at a constant porosity. Smaller size, angular shape, and more even distribution of particles increase the tortuosity of the paste.

- Slag and fly ash particles considerably decrease tortuosity; whereas silica fume incorporated pastes have almost the same tortuosity as OPC pastes. Superplasticizer addition significantly increases tortuosity through a better distribution of solid particles.

- The proposed model can adequately estimate the formation factor of fresh OPC paste mixtures with fly ash, silica fume, slag or superplasticizer. The formation factor-time

curve can be utilized as a new method to determine the initial setting time of cement-based materials.

It is recommended that the following topics are investigated further:

- The experimental tests of this study were conducted on cement paste. However, the presence of aggregates in concrete and mortar affect both the tortuosity and pore solution conductivity, which needs to be systematically studied.

- The cement used in this study was Type I or II Ordinary Portland Cement. The electrical resistivity characteristics of other types of cements (e.g. Type III or Type V) also need to be investigated.

- Only the effect of one type of super-plasticizer as a chemical admixture was included in this study. This can be further extended to other types of admixtures such as accelerators, retarders, corrosion inhibitors or air-entraining admixtures.

References

1. S.H. Kosmatka, M.L. Wilson, Design and Control of Concrete Mixtures, 16 ed., Portland Cement Association, Illinois, USA, 2016.

2. NRMCA, Ready Mixed Concrete Production Statistics, NAtional Ready Mix Concrete Association, Silver Spring, MD, 2016.

3. ASTM, ASTM C94: Standard Specification for Ready-Mixed Concrete, in: ASTM International (Ed.) ASTM C 94, ASTM International, West Conshocken, Pennsylvania, 2016.

4. J. Weiss, Relating Transport Properties to Performance in Concrete Pavements, in: S. Shields-Cook (Ed.) MAP - Moving Advancements into Practice, Federal Highway Admininstration, 2014, p. 6.

5. F. Presuel-Moreno, A. Suarez, Y. Lio, Characterization of New and Old Concrete Structures Using Surface Resistivity Measurements Florida Department of Transportation - Research Center, 2010, p. 263.

6. A. Jenkins, Surface Resistivity as an Alternative for Rapid Chloride Permeability Test of Hardened Concrete, Kansas Department of Transportation Bureau of Research, 2015, p. 39.

7. R.P. Spragg, J. Castro, T. Nantung, M. Paredes, W.J. Weiss, Variability Analysis of the Bulk Resistivity Measured Using Concrete Cylinders, Joint Transportation Research Program, Indiana Department of Transportation and Purdue University West Lafayette, IN, 2011, p. 13.

8. Session on Resistivity Measurements of Concrete Transportation Research Board Annual Meeting, Washington, D.C.

9. D.P. Bentz, K.A. Snyder, A. Ahmed, Anticipating the Setting Time of High-Volume Fly Ash Concretes Using Electrical Measurements: Feasibility Studies Using Pastes, J. Mater. Civ. Eng. (2014).

10. M. Mancio, J.R. Moore, Z. Brooks, P.J. Monteiro, S.D. Glaser, Instantaneous Determination of Water-Cement Ratio of Fresh Concrete, ACI Mater. J. 107(6) (2010).

11. X. Wei, L. Xiao, Influence of the aggregate volume on the electrical resistivity and properties of portland cement concretes, Journal of Wuhan University of Technology-Mater. Sci. Ed. 26(5) (2011) 965-971.

12. H. Whittington, J. McCarter, M. Forde, The conduction of electricity through concrete, Mag Concrete Res 33(114) (1981) 48-60.

13. Z. Li, X. Wei, W. Li, Preliminary interpretation of Portland cement hydration process using resistivity measurements, ACI Mater. J. 100(3) (2003).

14. X. Wei, Z. Li, Early hydration process of Portland cement paste by electrical measurement, J. Mater. Civ. Eng. 18(1) (2006) 99-105.

15. H. Sallehi, Characterization of Cement Paste in Fresh State Using Electrical Resistivity Technique, Civil and Environemntal Engineering, Carletn University, Ottawa, Canada, 2015, p. 200.

16. L. Xiao, Z. Li, Early-age hydration of fresh concrete monitored by non-contact electrical resistivity measurement, Cement and Concrete Research 38(3) (2008) 312-319.

17. J.C. Maxwell, Electricity and magnetism, Oxford University Press, Oxford, 1904.

18. H. Fricke, The electric conductivity and capacity of disperse systems, Journal of Applied Physics 1(2) (1931) 106-115.

19. E. Hammond, T. Robson, Comparison of electrical properties of various cements and concretes, The Engineer 199(5156) (1955) 114.

20. B. Hughes, A. Soleit, R. Brierley, New technique for determining the electrical resistivity of concrete, Magazine of concrete research 37(133) (1985) 243-248.

21. P. Longuet, L. Burglen, A. Zelwer, The liquid phase of hydrated cement, des Materiaux de Construction et de Travaux Pubics 676 (1973) 35-41.

22. D. Maguire, M. Olen, Report on an investigation into the electrical properties of concrete, Transactions of the South African Institute of Electrical Engineers 31 (1940) 301.

23. S.J. Pirson, Electric logging factors which affect true formation resistivities Oil and Gas Journal 46(26) (1947) 76-81.

24. A. Slawinski, Conductivity of an Electrolyte Containing Dielectric Bodies, Jour. Chem. Phys 23 (1926) 710-727.

25. G.E. Monfore, The electrical resistivity of concrete, Journal of the PCA Research and Development Laboratories 10(2) (1968) 35-48.

26. G.E. Archie, The electrical resistivity log as an aid in determining some reservoir characteristics, Transactions of the American Institute of Mining and Metallurgical Engineers 146 (1942) 54-62.

27. E. Atkins Jr, G. Smith, The significance of particle shape in formation resistivity factor-porosity relationships, Journal of Petroleum Technology 13(03) (1961) 285-291.

28. N. Neithalath, J. Jain, Relating rapid chloride transport parameters of concretes to microstructural features extracted from electrical impedance, Cement and Concrete Research 40(7) (2010) 1041-1051.

29. T.O. Mason, M.A. Campo, A.D. Hixson, L.Y. Woo, Impedance spectroscopy of fiber-reinforced cement composites, Cement Concrete Comp 24(5) (2002) 457-465.

30. T. Chrisp, G. Starrs, W. McCarter, E. Rouchotas, J. Blewett, Temperature-conductivity relationships for concrete: An activation energy approach, Journal of materials science letters 20(12) (2001) 1085-1087.

31. Y. Liu, F.J. Presuel-Moreno, Normalization of Temperature Effect on Concrete Resistivity by Method Using Arrhenius Law (with Appendix), ACI Materials Journal 111(1-6) (2014).

32. W. McCarter, T. Chrisp, G. Starrs, P. Basheer, J. Blewett, Field monitoring of electrical conductivity of cover-zone concrete, Cement and Concrete Composites 27(7) (2005) 809-817.

33. M.S. Morsy, Effect of temperature on electrical conductivity of blended cement pastes, Cement and concrete research 29(4) (1999) 603-606.

34. Y. Villagrán Zaccardi, J. Fullea García, P. Huelamo, A. Di Maio, Influence of temperature and humidity on Portland cement mortar resistivity monitored with inner sensors, Materials and corrosion 60(4) (2009) 294-299.

35. H. Sallehi, Characterization of Cement Paste in Fresh State Using Electrical Resistivity Technique, Civil and Environmental Engineering, Carleton university, 2015.

36. G. Sant, F. Rajabipour, P. Fishman, P. Lura, J. Weiss, Electrical conductivity measurements in cement paste at early ages: a discussion of the contribution of pore solution conductivity, volume, and connectivity to the overall electrical response, -Int. RILEM Workshop on Advanced Testing of Fresh Cementitious Materials, 2006.

37. Z. Li, L. Xiao, X. Wei, Determination of concrete setting time using electrical resistivity measurement, Journal of materials in civil engineering 19(5) (2007) 423-427.

38. H. Wojtas, Determination of polarization resistance of reinforcement with a sensorized guard ring: Analysis of errors, Corrosion 60(4) (2004) 414-420.